NRC "KURCHATOV INSTITUTE"
KURCHATOV NUCLEAR POWER COMPLEX

Capabilities of the GRUCON code package in the TSL data processing

Sinitsa V.V., Listov A.S., Zhukov V.A.
sinitsa_vv@nrcki.ru

Technical Meeting on the Nuclear Data Processing
18-22 October 2021, IAEA, Vienna, Austria

Topics

1. **GRUCON data structures and functional modules for the TSL data processing**

2. **Comparison of the ACE files prepared by GRUCON and NJOY**

3. **Comparison of results for ICSBEP benchmarks**

Conclusion

The Data Structures used in the THL Data Processing

Evaluated data
TH - incoherent inelastic scattering data
TI - incoherent elastic scattering data
TC - coherent elastic scattering data

Reconstructed data
S - integral cross sections
D - energy/angle distribution tables with point-wise initial energies
and variety of outgoing energy and angle representations

Group averaged data
F - group cross-sections
M - group transition matrices

GRUCON Processing Modules

*TH/-DS reconstructs of the *S* and *D* structures from
TH, *TI*,*TC* data for bound nuclei and from
elastic cross sections *S* (MT2) for free nuclei

*S/T-DS prepares of the *S* and *D* structures from
S (MT2) cross sections for given temperatures
in the free gas and resonance scattering models

*D/E-D converts continuous energy distributions of scattered
neutrons to discrete form (averaged in group intervals,
equally-likely energies)

*D/A-D changes angle distribution representation mode
(tabulated continuous dependency from cosine,
averaged in equal intervals, Legendre expansion
coefficients, equally-likely cosines)

Input / Output Modules

*ENDF reads data from the ENDF MF7 file and converts them to the *TH*,*TI* and *TC* structures

*PENDF reads/writes *S* and *D* structures from/to the NJOY internal PENDF MF3, MF6 files

*GENDF reads/writes *F* and *M* structures from/to the NJOY internal GENDF MF3, MF6 files

*ACE converts *S* and *D* structures to the ACE thermal scattering data file

*MATXS converts *F* and *M* structures to the MATXS format for TRANSX code to connect with transport SN codes

*CCCC coverts *F* and *M* structures to the CCCC/ISOTXS extended format for C4P processing code (KIT Karlsruhe)

Input deck for preparation of ACE file with data H in H2O

adaptive energy grid, equally-likely discrete cosines and energies

```
,in              ! enter local parameters
,in,1,endf       ! enter control parameters
,in,2,th/-ds     !
,in,3,ace        !
,1,20,th         ! read TSL data from the ENDF MF7 file
20,2,21,ds       ! reconstruct cross sections and energy/angle distributions
21,3,,H_H2O  ! prepare ace file
,,,end
!  -------------- local parameters -------------
*mtref:222,
*natom:2,
*niza:1,
*miza:1001,
*de:1.e-5,4.0,
*nt:16,
*tem:283.6,293.6,300.0,323.6,350.0,373.6,400.,423.6,450.,473.6,
        500.,523.6,560.,573.6,600.,623.6,
*eps:0.001
! ------------   control parameters ------------
*endf:ntape=20,nmat=0,nmf=1,nmt=0,mf=7
*th/-ds:*mtref,iset=0,*natom,nint=2,*nt,nang=32,ntypa=4,
         *de,*eps,*tem
*ace:nace=50,nxsd=51,ntyp=2,*niza,nsuf=0,*nt,*mtref,nbine=64,ifeng=0,*miza,
        *de,*tem
```

(2) Comparison of the ACE file data, prepared by GRUCON and NJOY

The thermal scattering data for 8 materials from the ENDF/B-VIII.0 evaluated data library were processed through the NJOY-2016.62 and GRUCON-2021 (current version) processing systems and the thermal ACE files for Monte-Carlo calculations have been obtained.

The cross sections were obtained at fixed (NJOY) and adapted (GRUCON) energy grids for incident neutron energies.

The 32 equally-likely cosines representation for angular distributions and continuous representation for energy distributions of scattered neutron were used.

The comparison results of energy-angle distributions at the thermal energy point Eth=0.0253 eV are presented.

The PREPRO/PLOTTAB code (D.Cullen) has been used for plotting of comparison results.

TSL Materials and Reactions

Material ENDF/B-VIII.0	MAT	MTs	elastic
$H(H_2O)$	1	222	-
$H(CH_2)$	37	223	iel
Be(metal)	26	231,232	coh
Be(BeO)	31	233,234	coh
O(BeO)	46	237,238	coh
C(graphite)	31	229,230	coh
$H(ZrH_n)$	58	225,226	iel
$Zr(ZrH_n)$	7	235,236	iel

H (H2O) incoherent inelastic

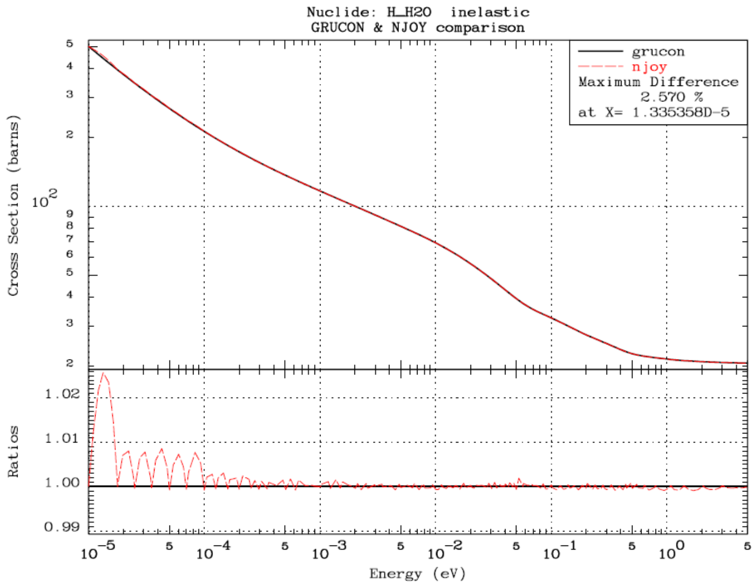

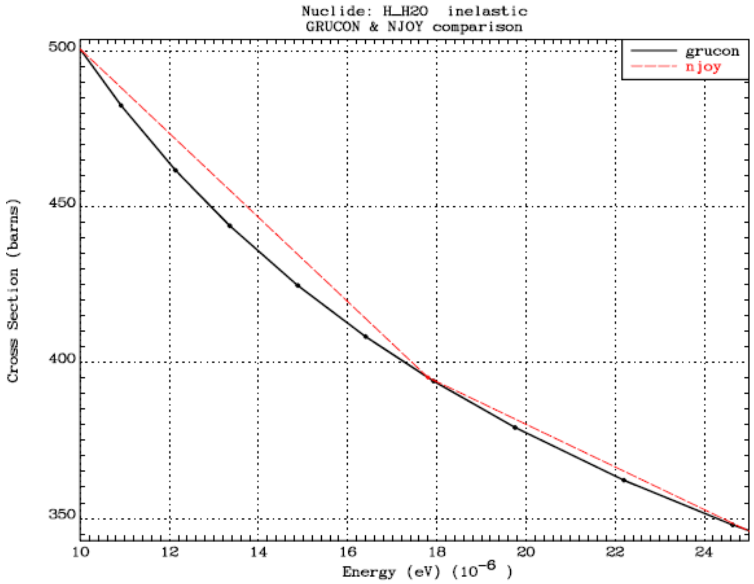

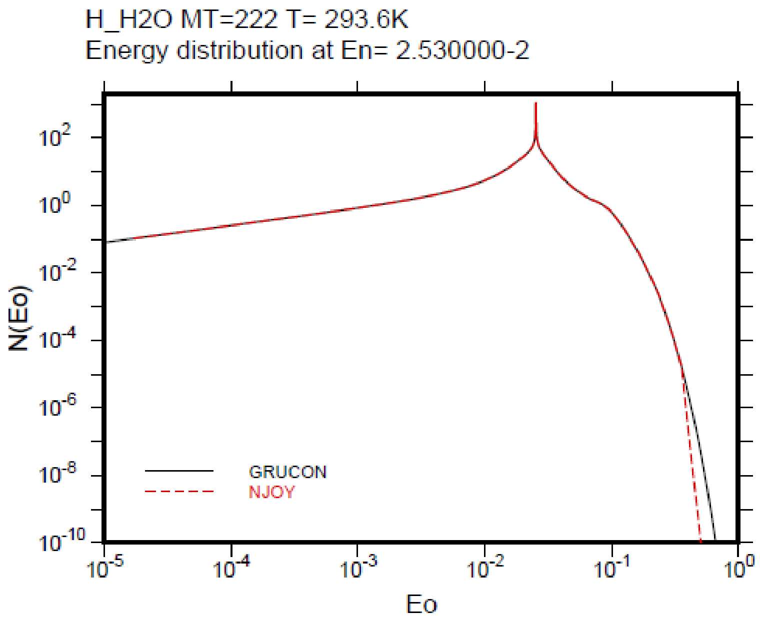

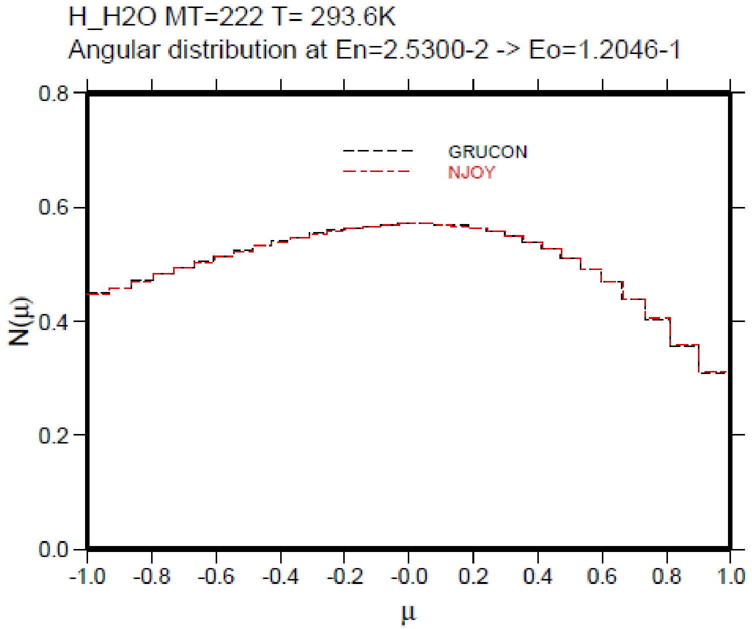

H (CH2) incoherent inelastic

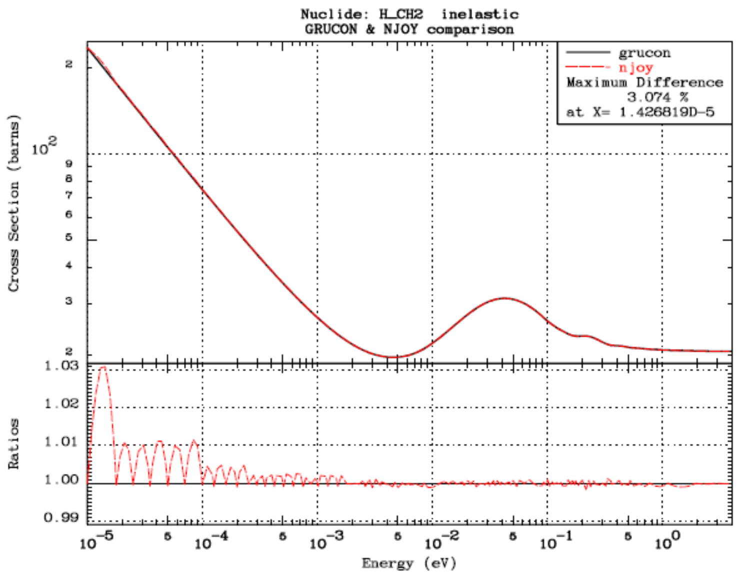

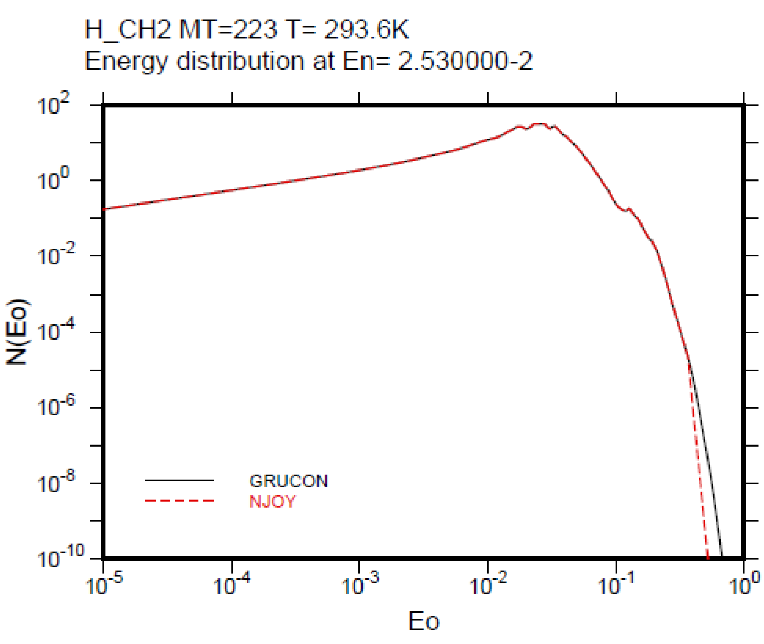

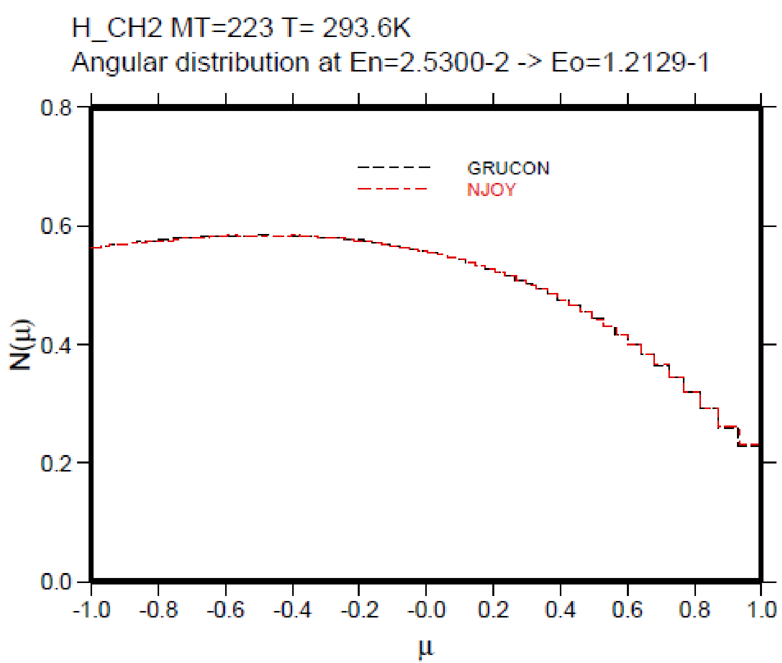

H (CH2) incoherent elastic

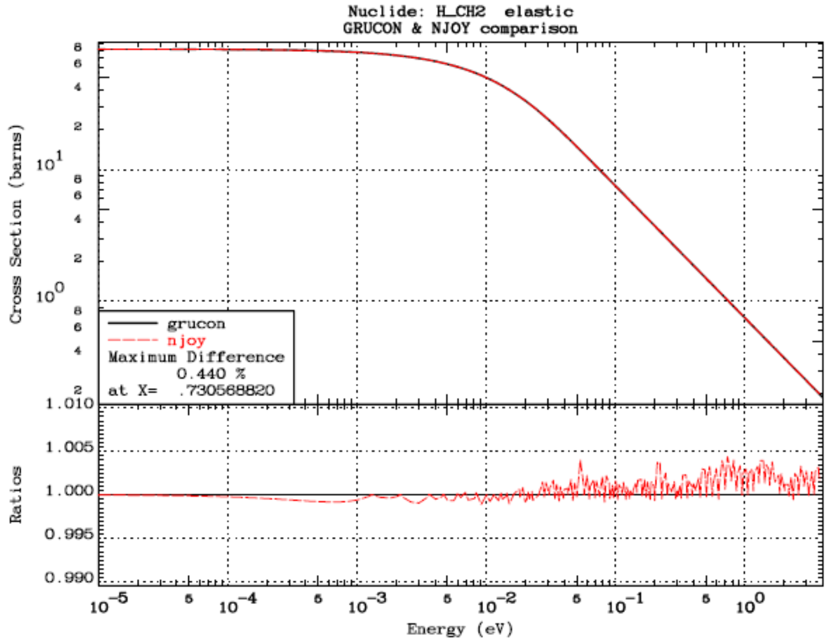

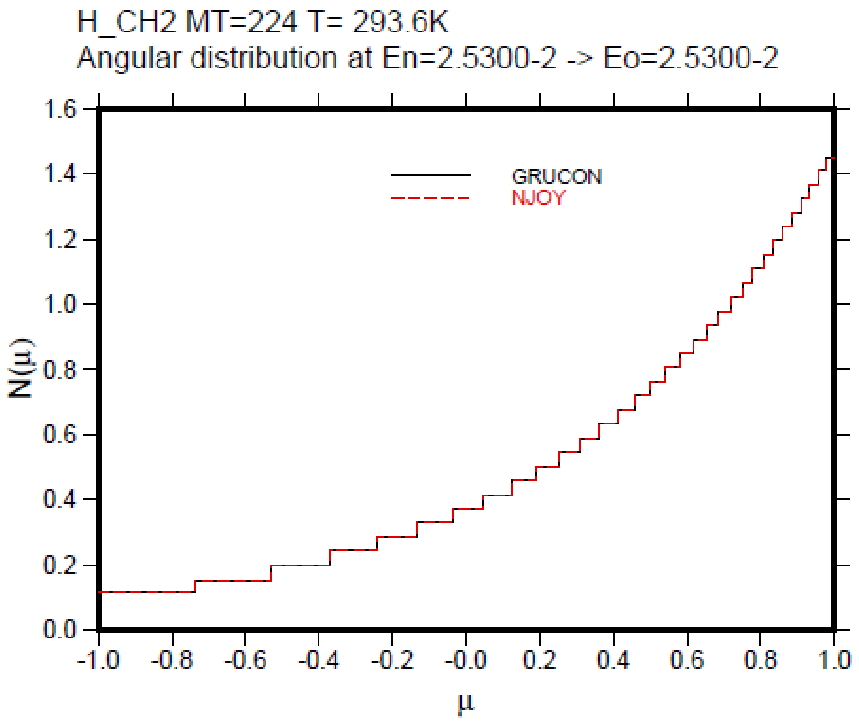

Be (metal) incoherent inelastic and coherent elastic

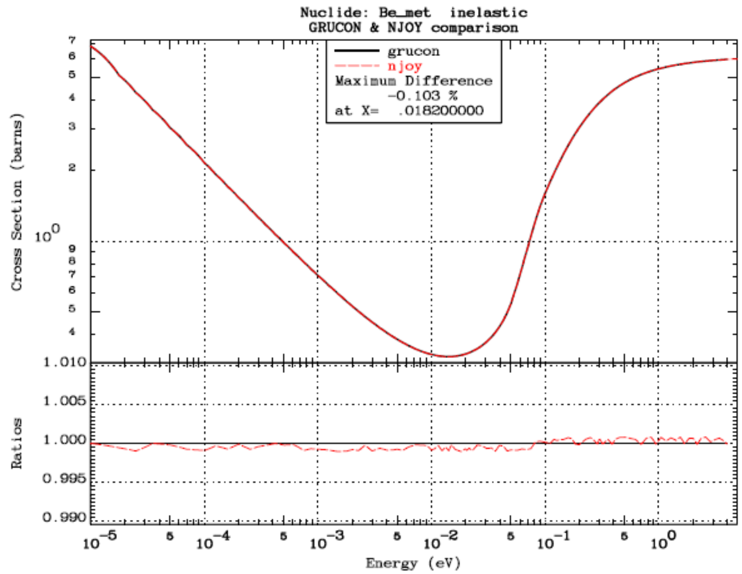

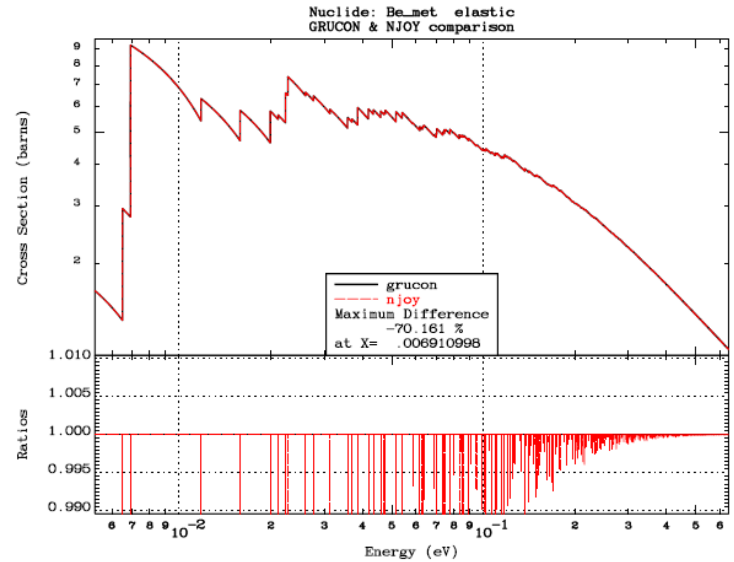

Be_met MT=231 T= 296.0K
Energy distribution at En= 2.530000-2

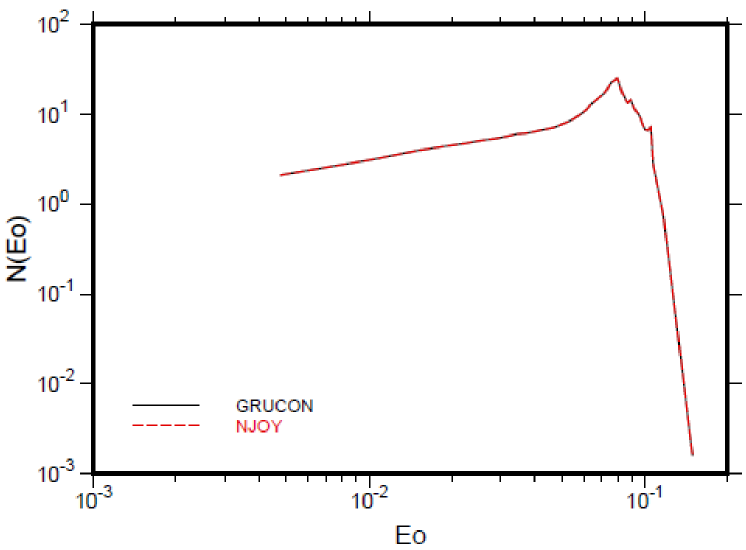

Be_met MT=231 T= 296.0K
Angular distribution at En=2.5300-2 -> Eo=1.4903-1

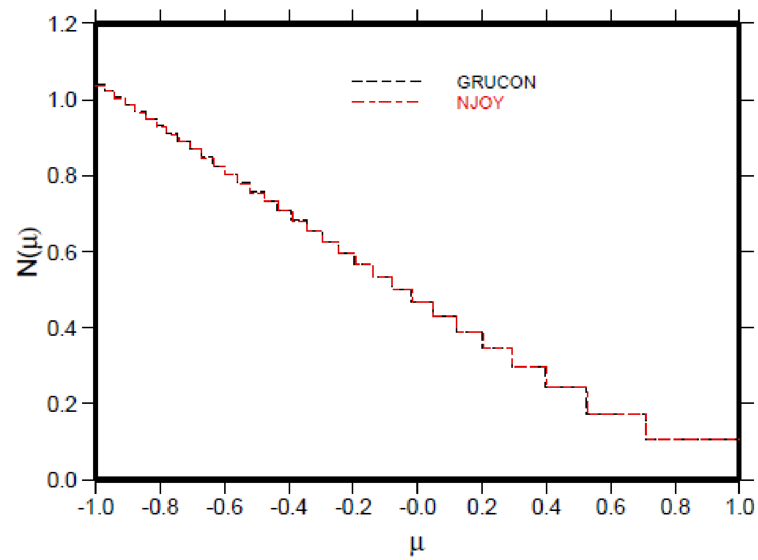

Be (BeO) incoherent inelastic and coherent elastic

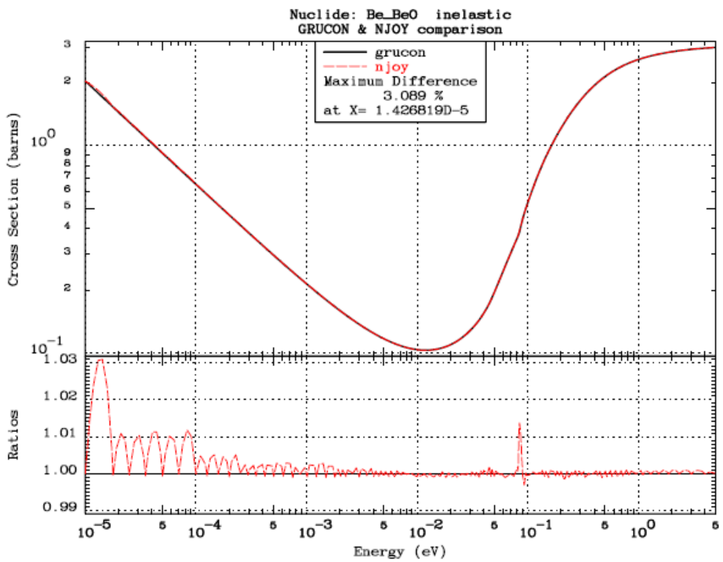

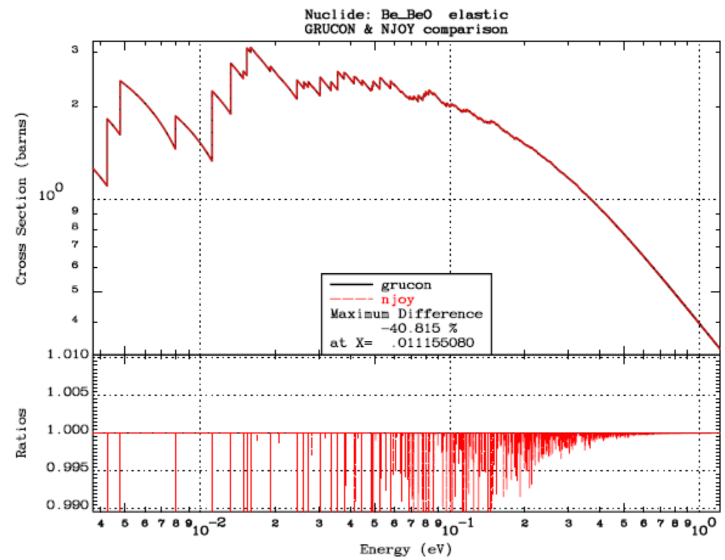

Be_met MT=231 T= 296.0K
Energy distribution at En= 2.530000-2

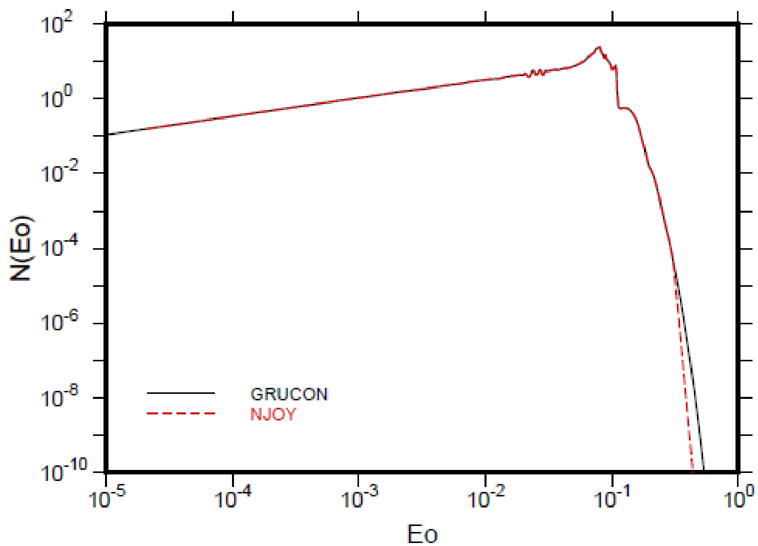

Be_BeO MT=233 T= 293.6K
Angle distribution at En=2.5300-2 -> Eo=1.5743-1

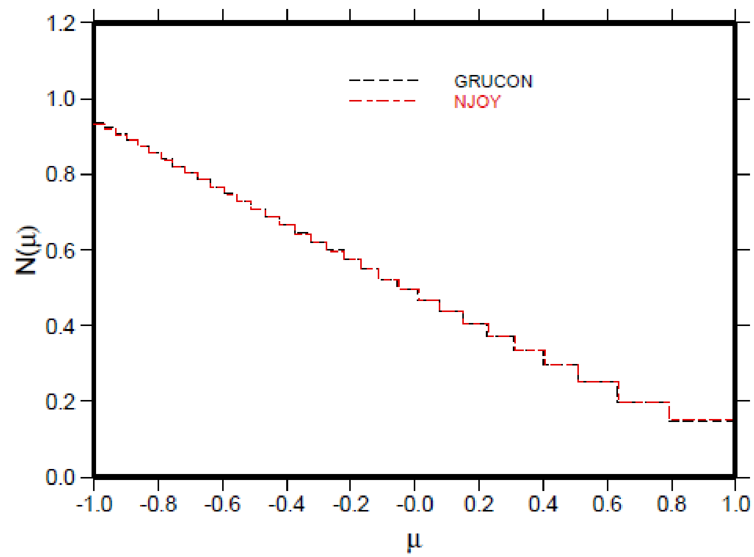

O (BeO) incoherent inelastic and coherent elastic

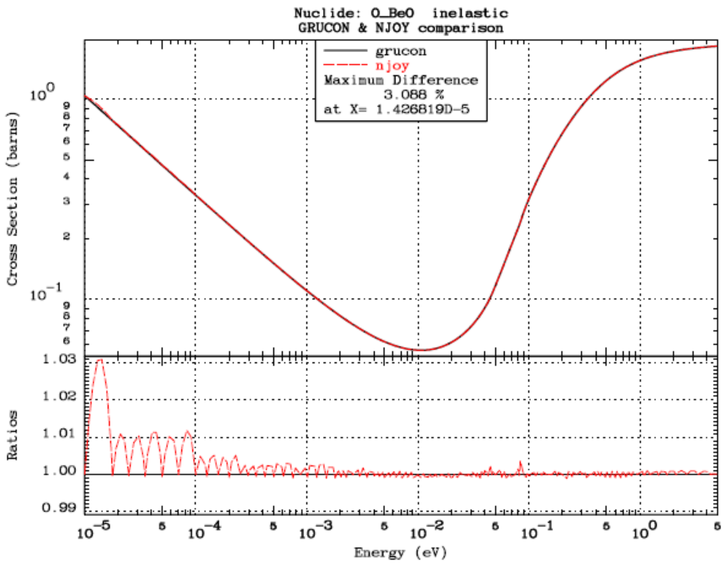

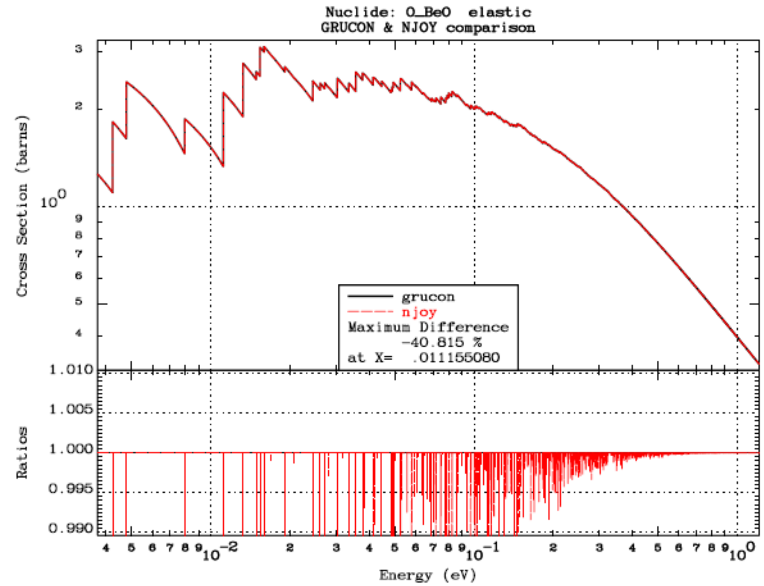

O_BeO MT=237 T= 293.6K
Energy distribution at En= 2.530000-2

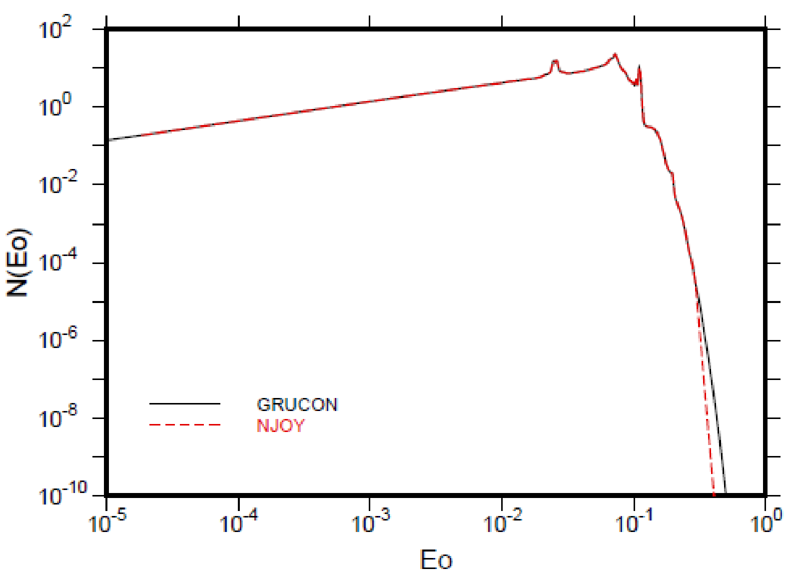

O_BeO MT=237 T= 293.6K
Angular distribution at En=2.5300-2 -> Eo=1.3752-1

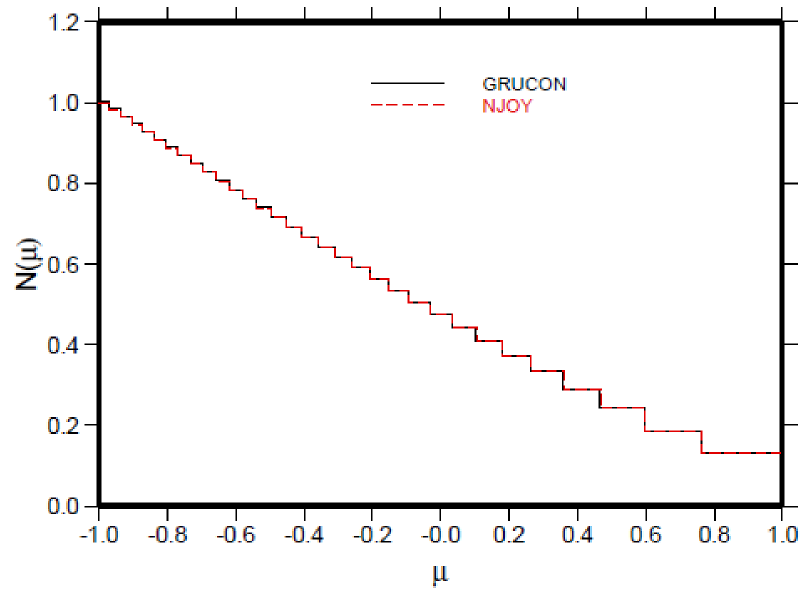

C (graphite) incoherent inelastic and coherent elastic

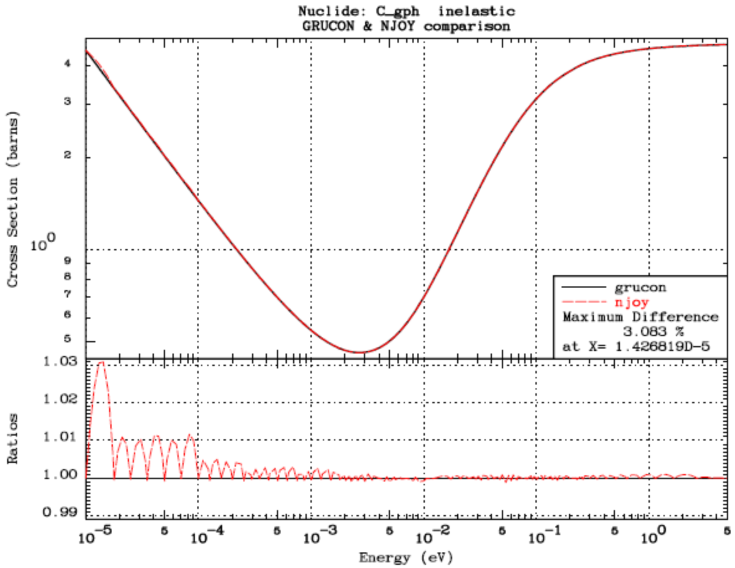

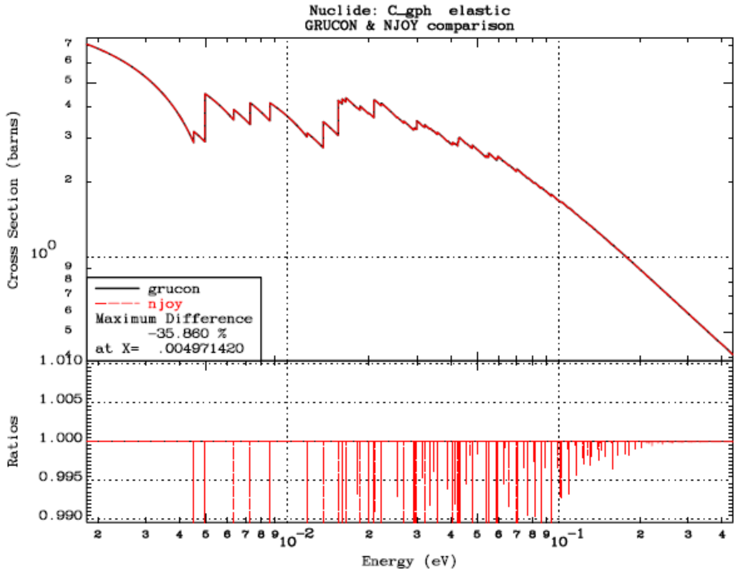

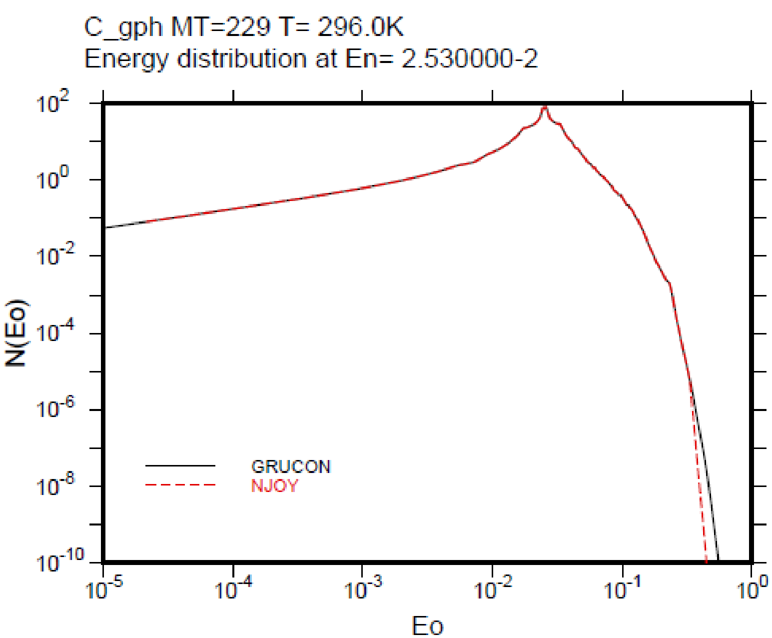

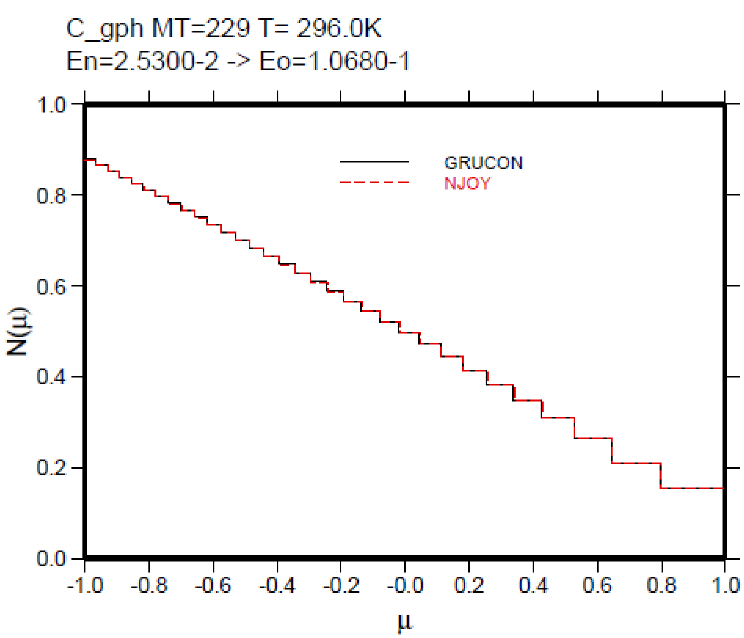

Zr (ZrH_n) incoherent inelastic

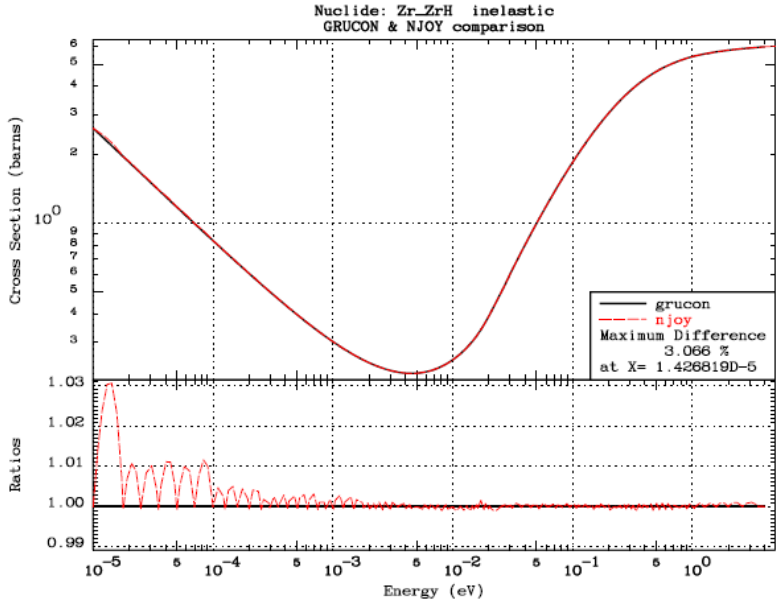

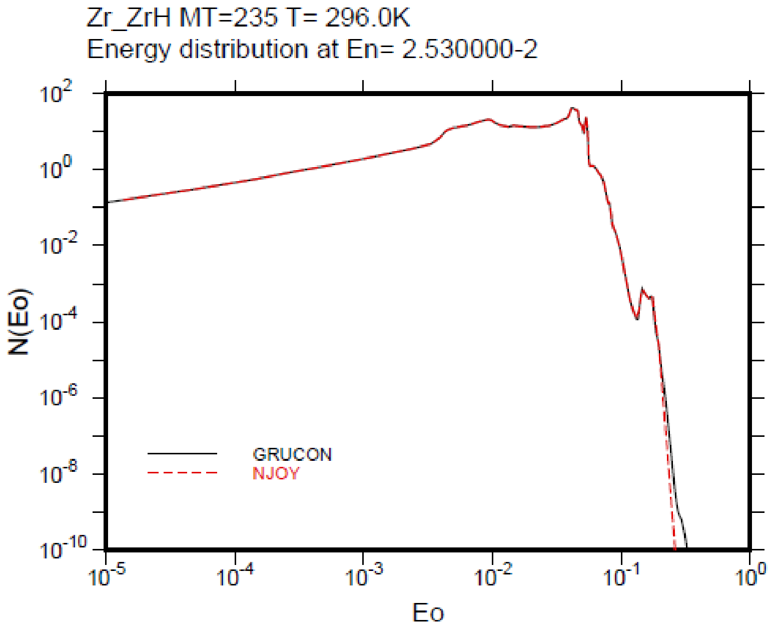

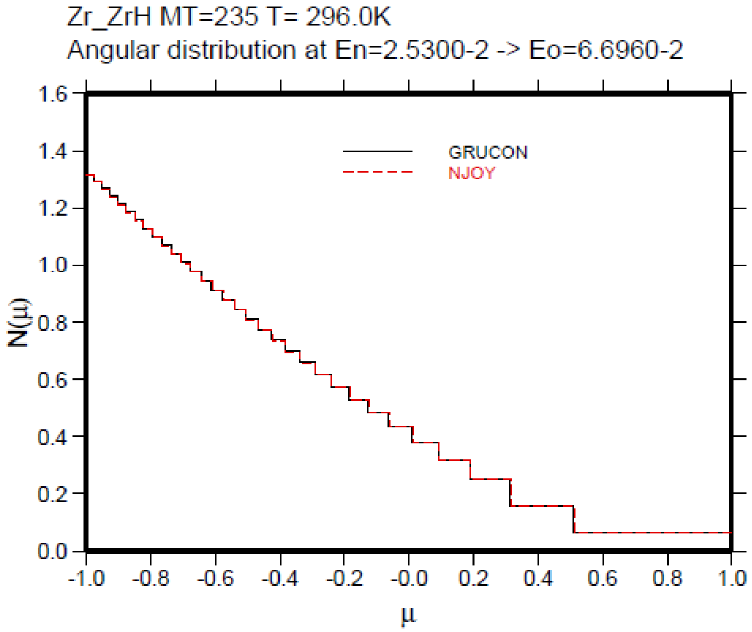

Zr (ZrH_n) incoherent elastic

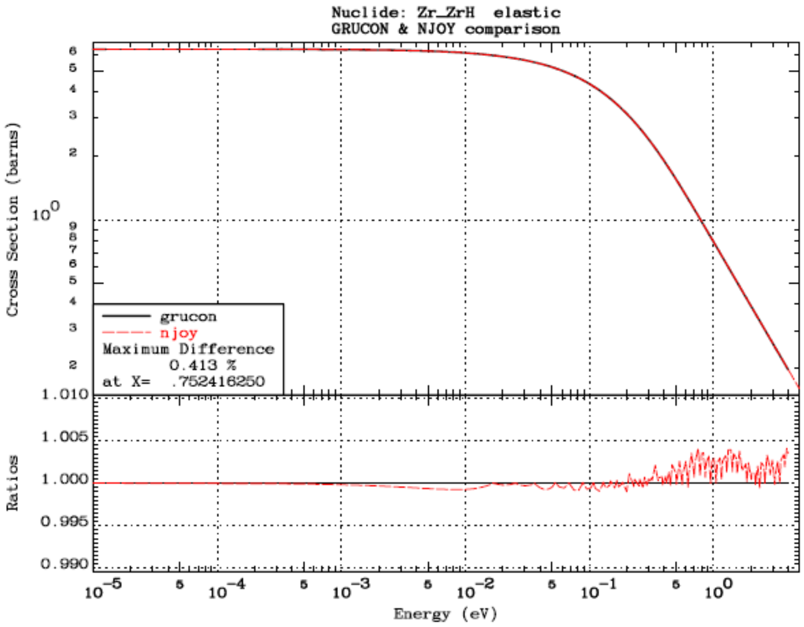

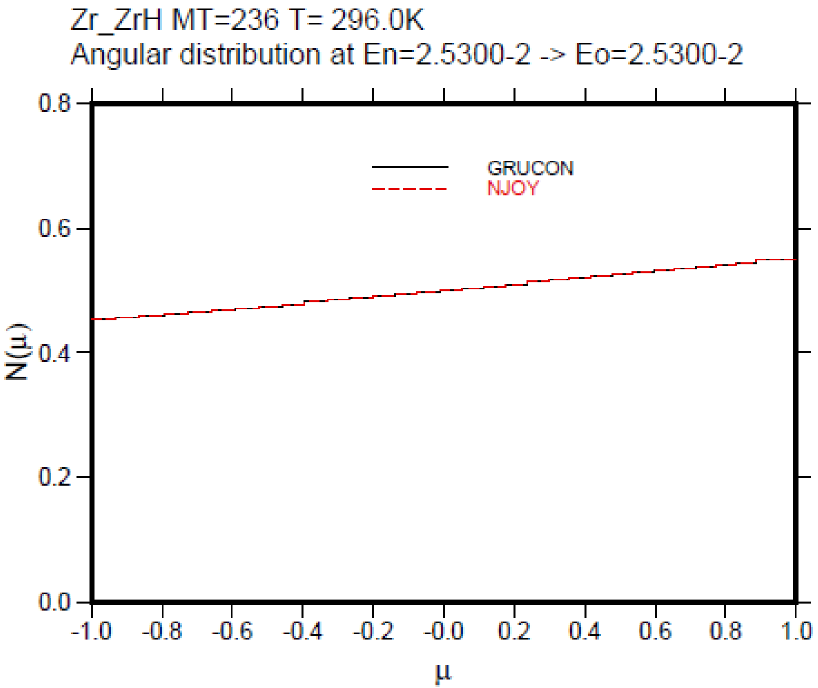

H (ZrH_n) incoherent inelastic

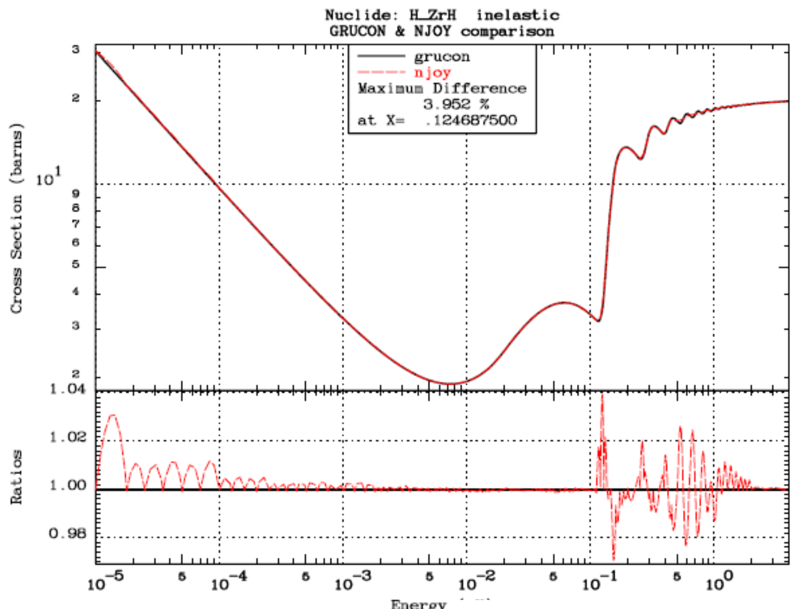

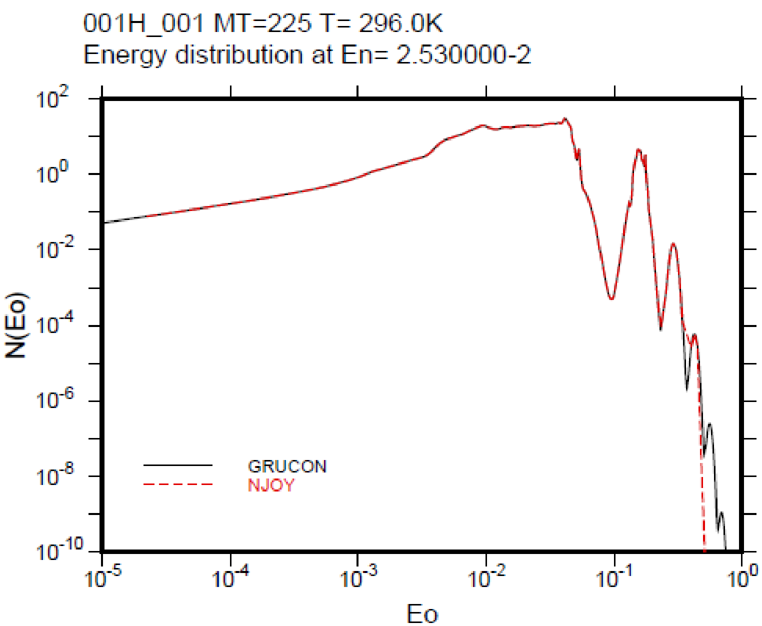

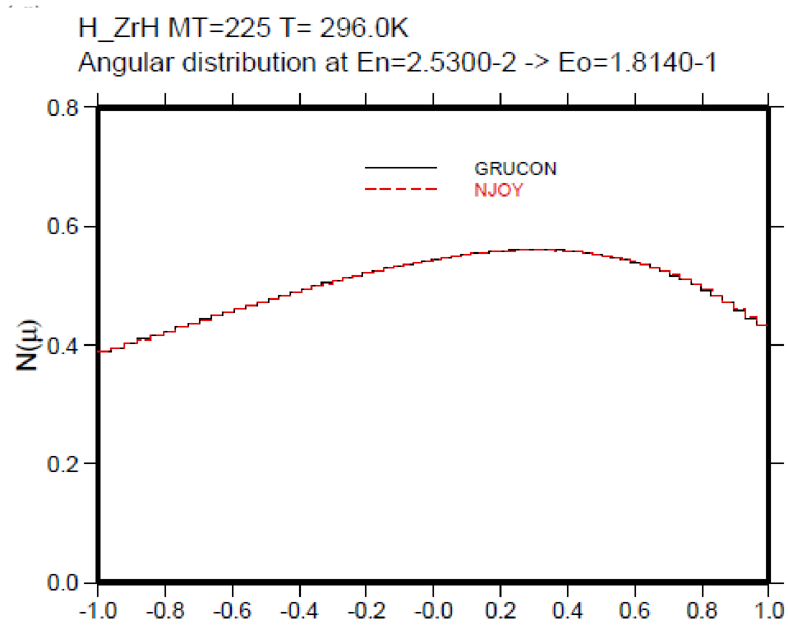

H (ZrH_n) incoherent elastic

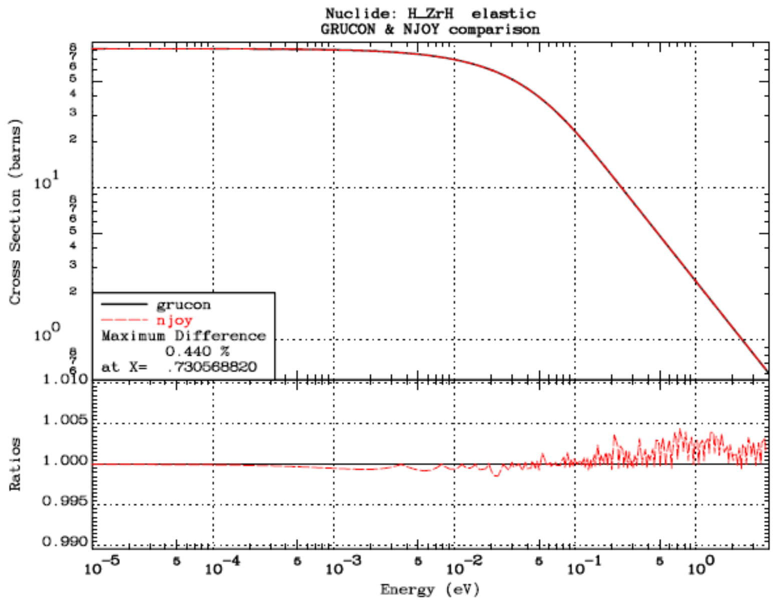

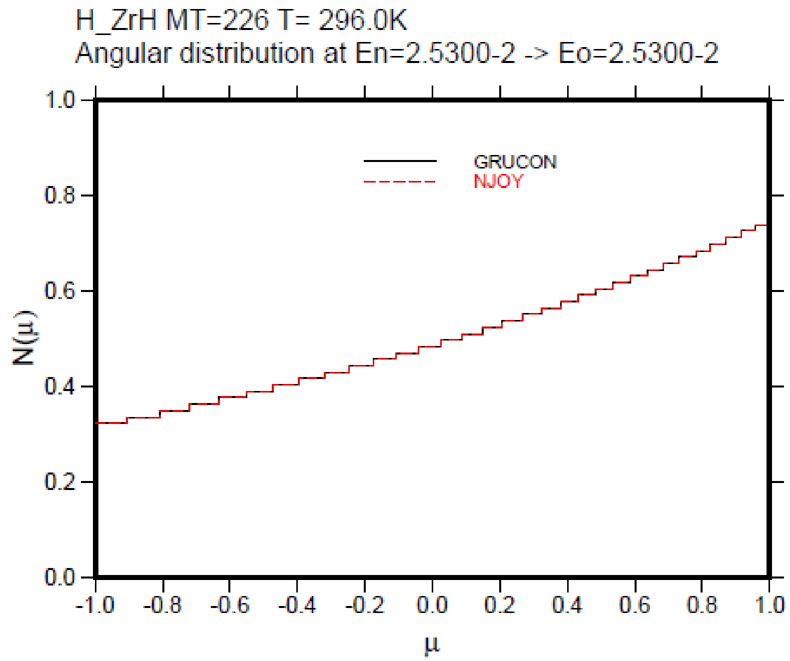

Comparison of energy distributions of scattered neutrons in discrete (64 bins with constant and skewed weights) and continuous representations (case H in ZrH)

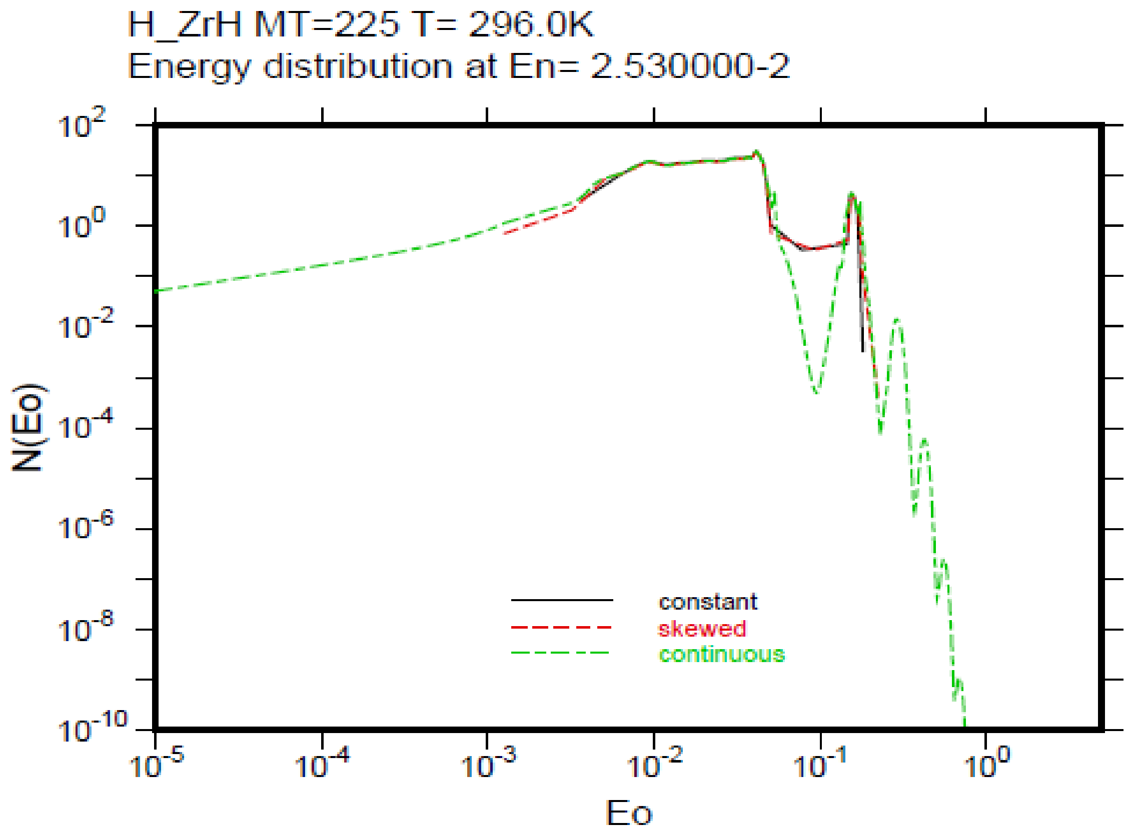

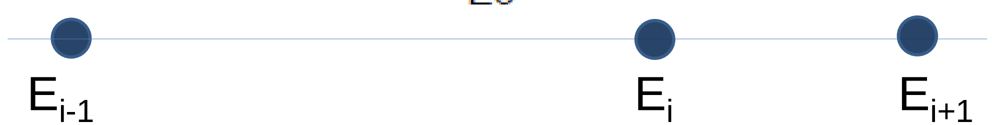

Probability density of equally-likely energy point E_i is defined here as $P_i = C/(E_{i+1}-E_{i-1})$,   where C – normalization factor

(3) Comparison of results for ICSBEP benchmarks

For integral testing of processed data, the ACE files for 123 (114 fast + 9 thermal) materials have been generated from the ENDF/B-VIII.0 evaluated data library by NJOY-2016.62 and GRUCON-2021 (current version) processing systems.

Three libraries were formed form these files, as follows:
ACE_NJOY – a library with files, prepared through NJOY,
ACE_GRUCON – a library with files, prepared through GRUCON,
ACE_MIXED(TSLMAT) – a temporary library, that was formed from the GRUCON ACE files except one, named TSLMAT, prepared through NJOY.

The thermal ACE files for this exercise were prepared at fixed energy grid (taken from NJOY) and with discrete representations of angle and energy distributions (32 and 64 bins, correspondingly) and with constant weights (IFENG=0). This was done to minimize influence of the thermal scattering data representation.
Calculations were performed for benchmarks from ICSBEP, that contain the TSLMAT material, with each of three ACE library.
The ratios to the Keff values obtained with ACE_GRUCON library were compared.

Benchmarks containing tested material

Material	List of the ICSBEP Benchmarks
H(H2O)	HSM-001 HSM-009_1 HSM-009_2 HSM-009_3 HSM-009_4 HSM-010_1 HSM-010_2 HSM-010_3 HSM-010_4 HSM-011_1 HSM-011_2 HSM-012 HSM-013_1 HSM-013_2 HSM-013_3 HSM-013_4 HSM-028_1 HSM-032 PSM-006_1 PSM-006_2 PSM-006_3 PSM-009_1a PSM-009_2a PSM-009_3a PSM-011_16_1 PSM-011_16_2 PSM-011_16_3 PSM-011_16_4 PSM-011_16_5 PSM-011_18_1 PSM-011_18_2 PSM-011_18_3 PSM-011_18_4 PSM-011_18_5 PSM-011_18_6 PSM-011_18_7 PSM-021_7 PSM-021_8 PSM-021_9
H(CH2)	MCT-008_1 MCT-008_2 MCT-008_3 MCT-008_4 MCT-008_5 MCT-008_6 MCT-008_3al MCT-008_3alc MCT-008_3b1 MCT-008_3b2 MCT-008_3b3 MCT-008_3b4 MCT-008_3cd MCT-008_3h1 MCT-008_3h2 MCT-008_3h3 MCT-008_3h4 MCT-008_3h5
C(graphite)	HCT-002_01 HCT-002_02 HCT-002_03 HCT-002_04 HCT-002_05 HCT-002_06 HCT-002_07 HCT-002_08 HCT-002_09 HCT-002_10 HCT-002_11 HCT-002_12 HCT-002_13 HCT-002_14 HCT-002_15 HCT-002_16 HCT-002_17 HCT-002_18 HCT-002_19 HCT-002_20 HCT-002_21 HCT-002_22 HCT-002_23 HCT-002_24 HCT-002_25
Be(metal)	HCM-003
Be(BeO)	HCM-003
O(BeO)	HCM-003
Zr(ZrH_n)	HCM-003 HCT-007-001cyl HCT-007-002cyl HCT-007-003cyl ICT-003-001
H(ZrH_n)	HCM-003 HCT-007-001cyl HCT-007-002cyl HCT-007-003cyl ICT-003-001

H (H2O)

1	HST-001_1
2	HST-009_1
3	HST-009_2
4	HST-009_3
5	HST-009_4
6	HST-010_1
7	HST-010_2
8	HST-010_3
9	HST-010_4
10	HST-011_1
11	HST-011_2
12	HST-012
13	HST-013_1
14	HST-013_2
15	HST-013_3
16	HST-013_4
17	HST-028_1
18	HST-032

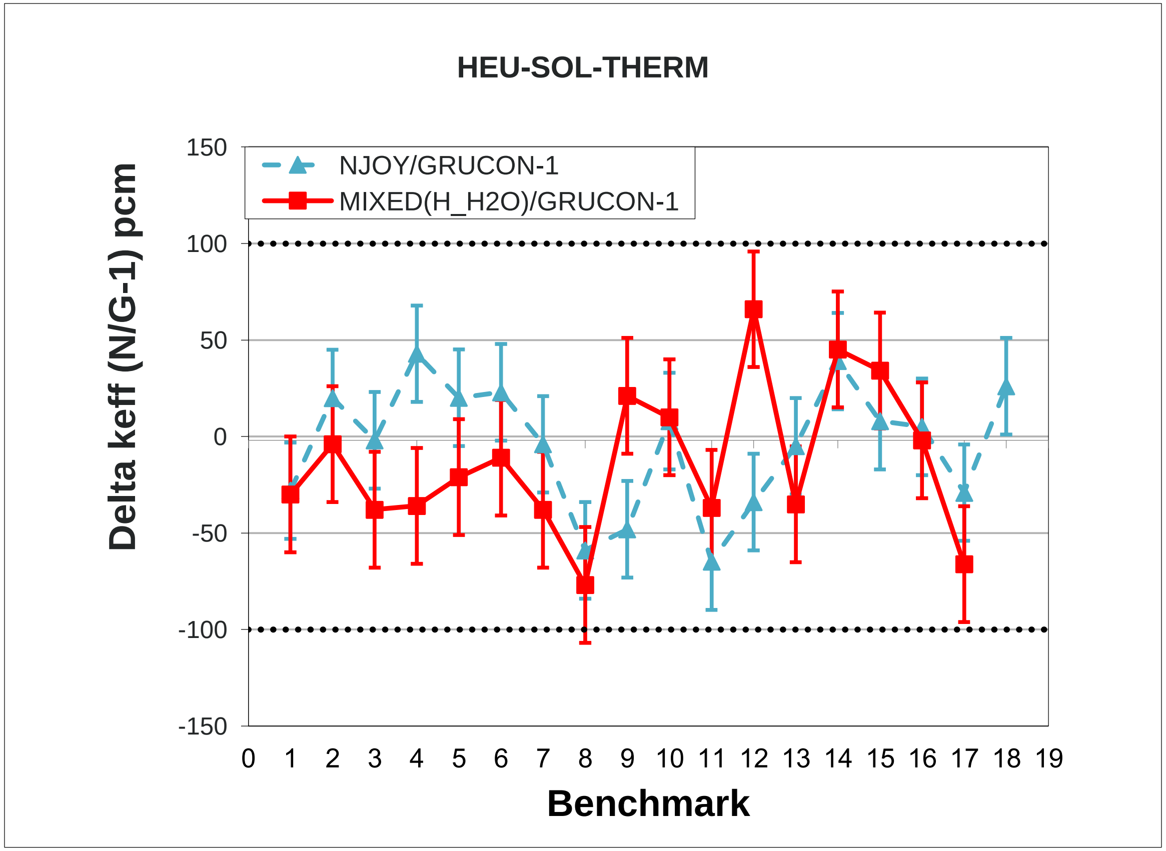

H (H2O)

1	PST-006_1
2	PST-006_2
3	PST-006_3
4	PST-009_1A
5	PST-009_2A
6	PST-009_3A
7	PST-011_16_1
8	PST-011_16_2
9	PST-011_16_3
10	PST-011_16_4
11	PST-011_16_5
12	PST-011_18_1
13	PST-011_18_2
14	PST-011_18_3
15	PST-011_18_4
16	PST-011_18_5
17	PST-011_18_6
18	PST-011_18_7
19	PST-021_7
20	PST-021_8
21	PST-021_9

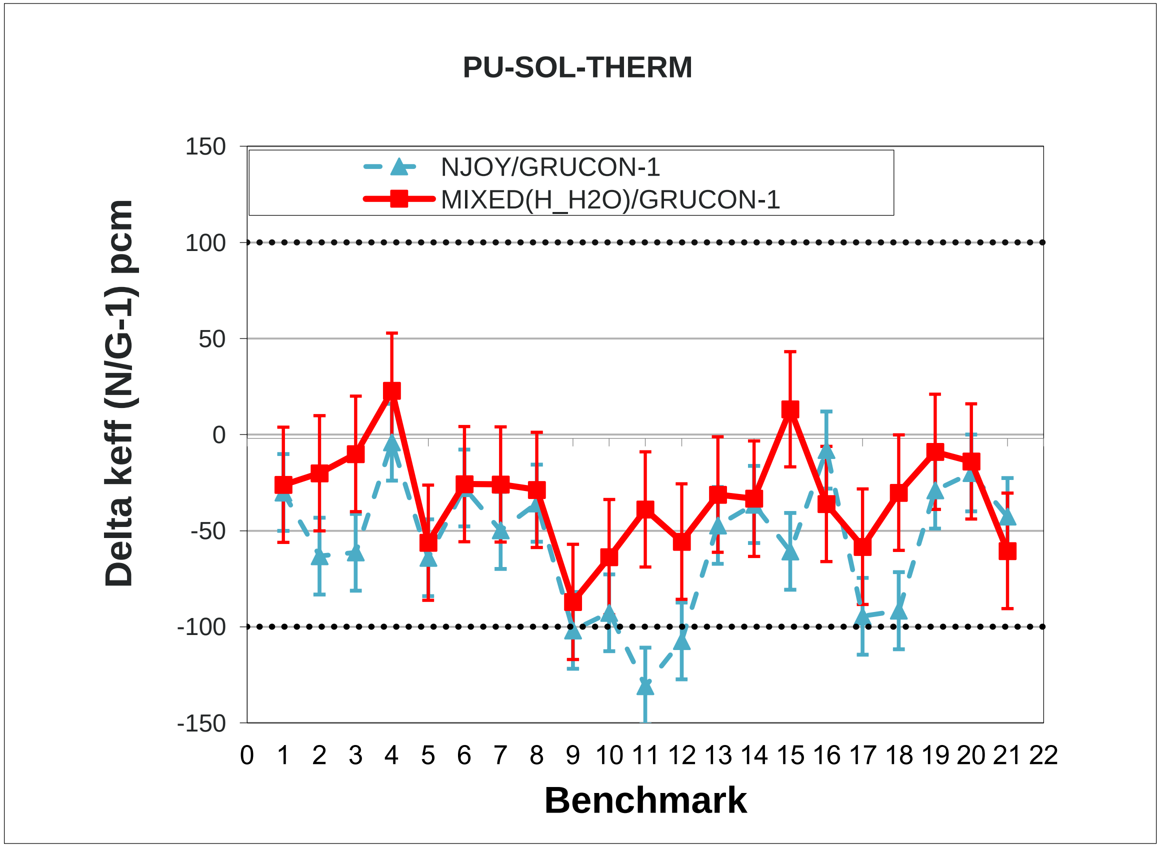

H (CH2)

1	MCT-008_1
2	MCT-008_2
3	MCT-008_3
4	MCT-008_4
5	MCT-008_5
6	MCT-008_6
7	MCT-008_3AL
8	MCT-008_3ALC
9	MCT-008_3B1
10	MCT-008_3B2
11	MCT-008_3B3
12	MCT-008_3B4
13	MCT-008_3CD
14	MCT-008_3H1
15	MCT-008_3H2
16	MCT-008_3H3
17	MCT-008_3H4
18	MCT-008_3H5

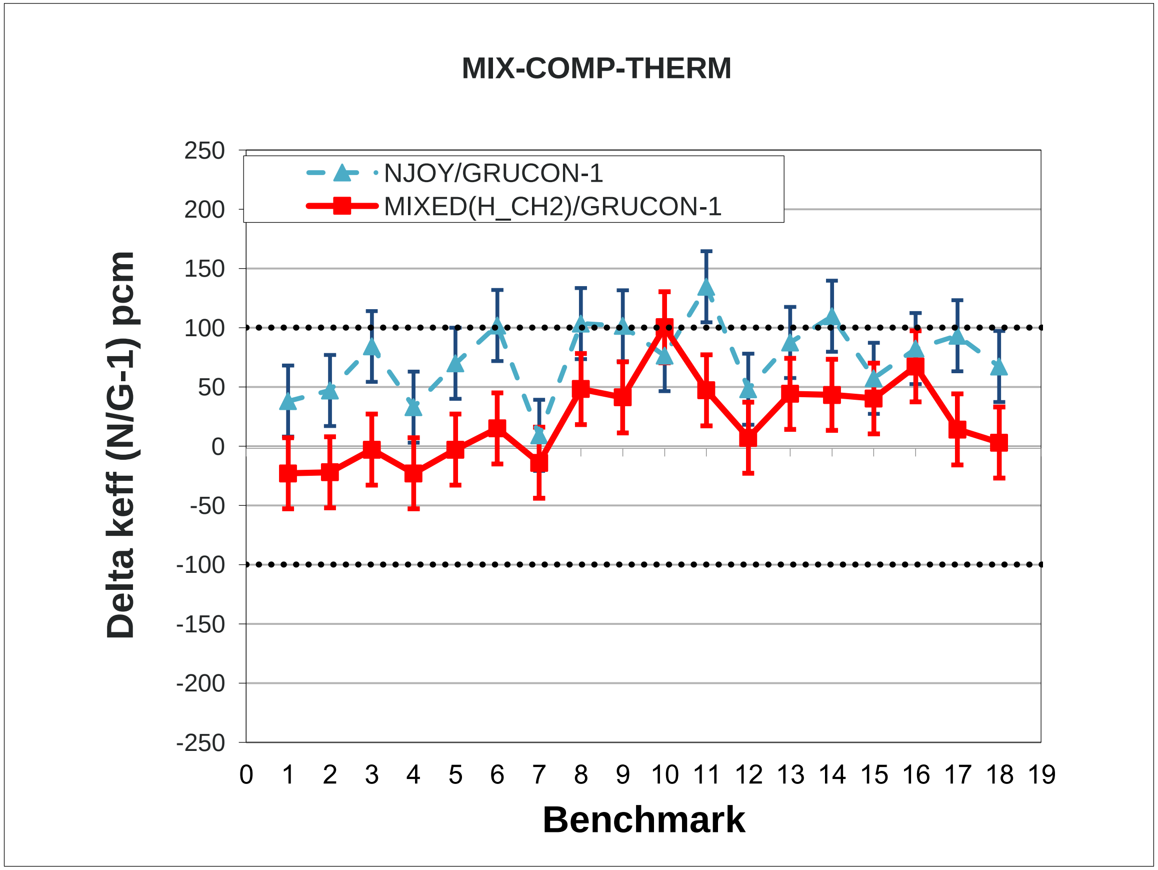

C (graphite)

1	HCT-2_1
2	HCT-2_2
3	HCT-2_3
4	HCT-2_4
5	HCT-2_5
6	HCT-2_6
7	HCT-2_7
8	HCT-2_8
9	HCT-2_9
10	HCT-2_10
11	HCT-2_11
12	HCT-2_12
13	HCT-2_13
14	HCT-2_14
15	HCT-2_15
16	HCT-2_16
17	HCT-2_17
18	HCT-2_18
19	HCT-2_19
20	HCT-2_20
21	HCT-2_21
22	HCT-2_22
23	HCT-2_23
24	HCT-2_24
25	HCT-2_25

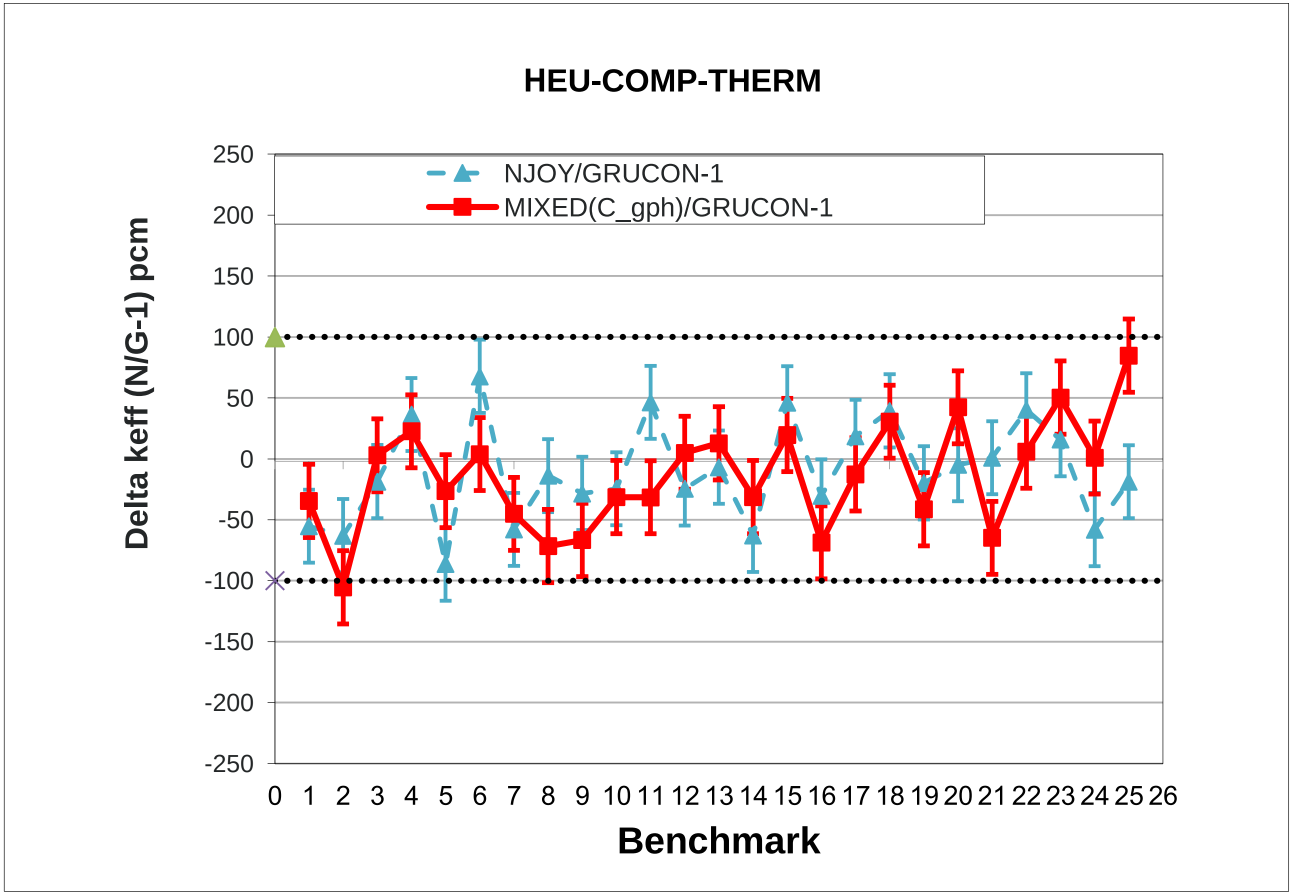

H(ZrH$_n$) & Zr(ZrH$_n$)

1	HCM-3_1
2	HCT-7_1C
3	HCT-7_2C
4	HCT-7_3C
5	ICT-3_1

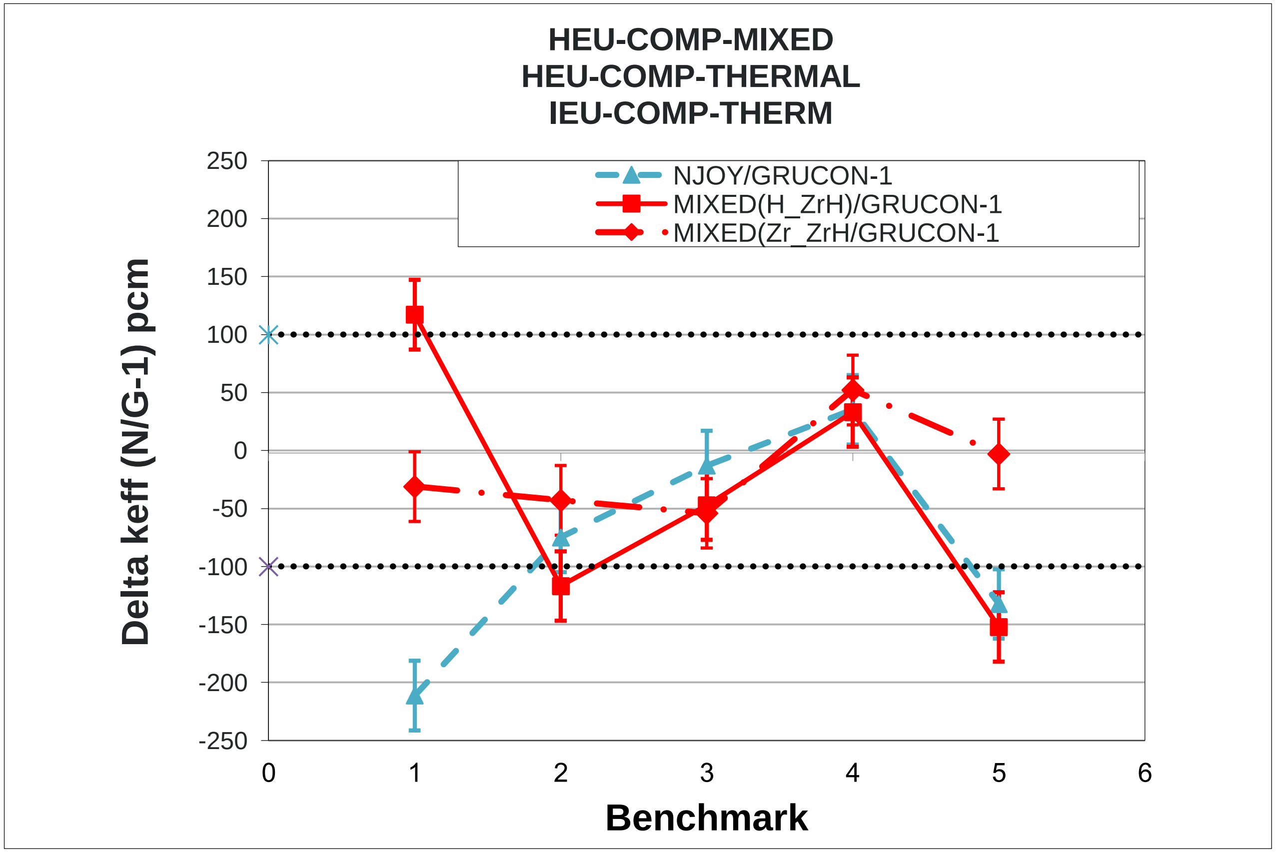

Conclusion

The GRUCON code allows to process the TSL data and prepare ACE files for detail calculation by the Monte-Carlo method in different representations, namely:

- fixed/adaptive energy grids for incident neutrons,
- discrete equally-likely cosines - for angular part,
- discrete equally-likely energies, obtained with constant or variable (skewed) weights, or tabulated continuous description - for energy part of energy-angular distribution of scattered neutrons.

Comparison of inelastic incoherent cross sections from the ACE files shown discrepancies up to 4% (case H in ZrH) due to the interpolation error of the fixed energy grid.
Comparison of incoherent elastic cross sections reveals no disagreements between fixed and adapted energy grids.
Differences in the coherent elastic cross sections are connected with tiny shifting of break energies and can be neglected.
As for energy and angular distributions, acceptable agreement is achieved between GRUCON and NJOY processing codes.
Comparison of benchmark calculation results demonstrates agreement within processing tolerance parameter eps=0.1% for cases, sensitive to the TSL data processing.

Thank you
for attention!